EUROPEAN ORGANIZATION FOR NUCLEAR RESEARCH

CERN-EP/88-34
15 March 1988

A-DEPENDENCE OF THE CHARM PRODUCTION CROSS-SECTION IN 300 GeV/c PROTON INTERACTIONS

WA78 Collaboration

H. Cobbaert and R. Roosen
Inter-University Institute for High Energies, ULB-VUB, Brussels, Belgium

M.G. Catanesi, M.T. Muciaccia, S. Natali, S. Nuzzo, M. Quattromini and F. Ruggieri
Università di Bari and INFN, Bari, Italy

G. Carboni[1], G. Crosetti[2], M. Fidecaro, C. Gerke[3], G. Poulard and H. Sletten
CERN, Geneva, Switzerland

M. Coupland, I.G. Roberts and P.T. Trent
Birkbeck College, London, UK

J.H. Bartley, J.E. Conboy, M.J. Esten, P. Fennel and P.F. Harrison
University College, London, UK

M. De Vincenzi, S. Di Liberto, A. Frenkel, M. Iori, E. Lamanna, G. Marini[4], G. Martellotti, A. Nigro, A. Parisi, G. Penso, S. Petrera, P. Pistilli[5], G. Romano[4], G. Rosa and A. Sciubba
Università di Roma 'La Sapienza' and INFN, Rome, Italy

B. Alessandro, V. Bisi, D. Gamba, L. Ramello and L. Riccati
Università di Torino and INFN, Turin, Italy

ABSTRACT

The A-dependence of the charm production cross-section is determined by measuring the yield of prompt single muons in a beam-dump experiment, using a 300 GeV/c proton beam on Al, Fe, and U targets. Assuming that the production cross-section varies as A^{α}, we obtain $\alpha(\mu^+) = 0.79 \pm 0.12$ and $\alpha(\mu^-) = 0.76 \pm 0.13$ in the kinematical region $x_F \gtrsim 0.1$ of the charm.

(Submitted to Physics Letters B)

Present addresses:
1) INFN, Pisa, Italy.
2) INFN, Genoa, Italy.
3) DESY, Hamburg, Fed. Rep. Germany.
4) Università di Salerno and INFN, Salerno, Italy.
5) Università di Lecce and INFN, Lecce, Italy.

We present an experimental comparison of the charm production cross-sections, measured at the CERN Super Proton Synchrotron (SPS) with a 300 GeV/c proton beam on three different materials: Al, Fe, and U. The charmed particles, produced in a variable-density target, are identified by detecting the prompt single muons coming from their semileptonic decays. Similar results, obtained with a 320 GeV/c π^- beam, have already been published [1].

The set-up (fig.1), which has been described in detail elsewhere [2], consists essentially of a variable-density target calorimeter, followed by a muon magnetic spectrometer. Upstream of the calorimeter, two beam counters (BC1 and BC2) and a veto wall (VW) define a beam particle through the coincidence

$$\mathrm{BEAM} = \mathrm{BC1} \cdot \mathrm{BC2} \cdot \overline{\mathrm{VW}} .$$

The spectrometer consists of a dipole superconducting magnet (1.5 T) equipped with drift and multiwire proportional chambers. This system enables us to measure the muon momentum with a resolution of $\Delta p/p = 6 \times 10^{-4} p$ (GeV/c).

The target calorimeter consists of 100 absorber plates interleaved with 100 plastic scintillator sheets, 5 mm thick. Light signals from every four consecutive scintillators are conveyed through optical fibres to a single photomultiplier. In this way the calorimeter is divided into 25 modules. The first 13 upstream modules form the target section, which is expandable and allows an easy change of the absorbers and of their density. The last 12 downstream modules, with iron absorbers, are kept fixed.

Single-muon and dimuon rates were measured with Al, Fe, and U targets at three different densities, corresponding to expansion factors of 1 (compact form), 1.5, and 2 (fully expanded form). By extrapolation to infinite density, we are able to deduce the prompt single-muon rate from which the charm signal is extracted. All 13 modules of the target section contain absorbers of the same material for the Fe and U runs, but in the case of Al, owing to its longer interaction length, only the first 5 modules of the target section contain Al absorbers, whilst the last 8 modules contain U. The different configurations of the calorimeter are reported in Table 1.

The muon trigger [2] requires at least one hit in each plane of the scintillator hodoscopes H1, H2, and H3, i.e.

$$\mathrm{BEAM} \cdot (\mathrm{H1Y} \geq 1) \cdot (\mathrm{H1Z} \geq 1) \cdot (\mathrm{H2} \geq 1) \cdot (\mathrm{H3} \geq 1) .$$

Beam muons were eliminated, for Fe and U data, by also requiring a coincidence with an interaction counter (IC) (fig. 1) with a threshold of $\sim$ 3 minimum ionizing particles. The IC was placed after the fifth module for Fe data, and after the seventh module for U data. For Al data, this rejection was made with a hardware processor which required an energy deposited in the calorimeter, $E_{\mathrm{cal}} \geq$ 80 GeV. In the off-line analysis this condition was also required for Fe and U data. Only events with at least one muon reconstructed in the spectrometer were retained, provided their momentum lay in the interval 20 GeV/c $\leq p_\mu \leq$ 100 GeV/c. This ensures a good spectrometer reconstruction. The pile-up effect of two beam particles in the calorimeter was eliminated by requiring that the energy deposited in the calorimeter be lower than 400 GeV, and that no other beam particles be present in the 150 ns preceding an accepted event and in the 80 ns following it. Finally, only those events in which the interaction took place in the second to fifth calorimeter modules (for Al and Fe data) or in the third to sixth modules (for U data) are included in the analysis. Events starting in the first module(s) were eliminated because of the calorimeter albedo, which can reach the veto wall counter, particularly when a U target is used. This cut also rejects upstream beam interactions, which appear as interactions in the first module.

With these selection criteria, the total number of effective interactions collected with Al, Fe, and U targets, are reported in table 2. For each material, data have been taken at three different densities of the target section of the calorimeter. The standard $1/\varrho \to 0$ extrapolation procedure was used to separate the prompt from the non-prompt muons which are produced by pion and kaon decays in the hadronic shower. Following the method already discussed in ref. [1], the non-prompt muons originating in the fixed part of the calorimeter have been estimated to be of the order of 2%. In fig. 2 we report the muon rate for single-muon and dimuon events, versus the inverse density of the expanded section of the calorimeter. As expected with an incident proton beam, the rate of non-prompt positive muons exceeds that of negative ones, contrary to what happens with a π^- beam [1]. Furthermore, for a proton beam the prompt muon rate is comparable for μ^+ and μ^-, whilst for a π^- beam, the prompt μ^- rate is definitely higher [1] than that of μ^+. These effects are in agreement with what was already observed and explained [1, 3, 4].

The dimuon rate (fig. 2), which is essentially due to the Drell–Yan process, is independent of target density, as expected. A fraction of these events in which one of the muons is not detected constitutes a prompt background in the single-muon channel, and therefore must be subtracted in order to get the net single-muon rate from charm decay. This fraction, which turns out to be ~ 24% of the observed prompt single-muon rate, has been evaluated by the Monte Carlo method, according to the parametrization of the inclusive muon pair-production cross-section reported in ref. [5].

In table 3 we report the single-muon rate from charm decay after all the corrections have been applied. For the Al data, the larger errors are due to the lower statistics combined with the special background subtraction method already described in ref. [1].

Figure 3 shows the kinematical acceptance of the experiment as a function of the Feynman x (x_F) of a charmed particle produced with a differential cross-section*)

$$\frac{d\sigma}{dp_T^2} \propto \exp(-1.1 p_T^2)$$

and undergoing a three-body (60%) or four-body (40%) semimuonic decay. Folding this acceptance with an x_F distribution

$$\frac{d\sigma}{dx_F} \propto (1 - |x_F|)^n,$$

with $n \simeq 5$ as suggested by the LEBC-EHS experiment [6], results in an x_F distribution with an average value of ~ 0.23 and a width of ~ 0.31 (FWHM). Therefore, in practice we are sensitive to x_F values $\gtrsim 0.1$. In fig. 4 we report the single-muon rate from charm decay as a function of the atomic number of the target. Parametrizing the charm production cross-section in the above-mentioned kinematical region as $\sigma_{c\bar{c}}(pA) = \sigma_0 A^\alpha$, the fitted slopes of fig. 4, combined with the A-dependence of the total absorption cross-section [7], lead to the following values: $\alpha(\mu^+) = 0.79 \pm 0.12$ and $\alpha(\mu^-) = 0.76 \pm 0.13$.

In conclusion: using a 300 GeV/c proton beam, we have measured the A-dependence of the charm production cross-section in the kinematical region $x_F \gtrsim 0.1$. Comparable α values have been obtained in previous charm production experiments, with pion [1], proton [8], and neutron [9], beams.

*) This p_T^2 distribution was also used in Ref. [1] but, owing to a printing error, it was not correctly reported there.

REFERENCES

[1] H. Cobbaert et al., Phys. Lett. **B191** (1987) 456.

[2] M.G. Catanesi et al., Nucl. Instrum. Methods **A253** (1987) 222.

[3] J.L. Ritchie et al., Phys. Lett. **B126** (1983) 499.

[4] J.L. Ritchie et al., Phys. Lett. **B138** (1984) 213.

[5] K.J. Anderson et al., Phys. Rev. Lett. **37** (1976) 799 and 803.

[6] M. Aguilar-Benitez et al., Phys. Lett. **B189** (1987) 476.

[7] A.S. Carroll et al., Phys. Lett. **B80** (1979) 319. Following this reference, we have taken for the total absorption cross-section of proton on nuclei, $\sigma_{abs} \propto A^{0.72}$.

[8] M.E. Duffy et al., Phys. Rev. Lett. **55** (1985) 1816.

[9] A.N. Aleev, Dubna Report D1-86-422 (1986).

Table 1
Summary of calorimeter configurations

Al target	Fe target	U target	
50 mm Al (× 20)	25 mm Fe (× 52)	10 mm U (× 20)	Expandable
15 mm U (× 32)		15 mm U (× 32)	Expandable
25 mm Fe (× 48)	25 mm Fe (× 48)	25 mm Fe (× 48)	Fixed

Table 2
Total effective number of interactions for the three targets

Target	Interactions
Al	6.1×10^{7}
Fe	2.1×10^{8}
U	2.0×10^{8}

Table 3
Corrected number of single-muon events from charm decay per 10^{6} effective interactions

Target	μ^{+}	μ^{-}
Al	20.5 ± 17.6	7.2 ± 13.6
Fe	32.7 ± 4.3	26.3 ± 3.7
U	36.0 ± 3.9	28.0 ± 3.4

Figure captions

Fig. 1 : Experimental set-up of the WA78 experiment with the calorimeter in compact form.

Fig. 2 : Single and dimuon rate for Al, Fe, and U targets versus the inverse density of the expanded section of the calorimeter; $\varrho = 1$ corresponds to the unexpanded situation.

Fig. 3 : Acceptance of the experiment versus x_F of a charmed particle.

Fig. 4 : Prompt single-muon rate from charm decay versus the atomic weight of the target.

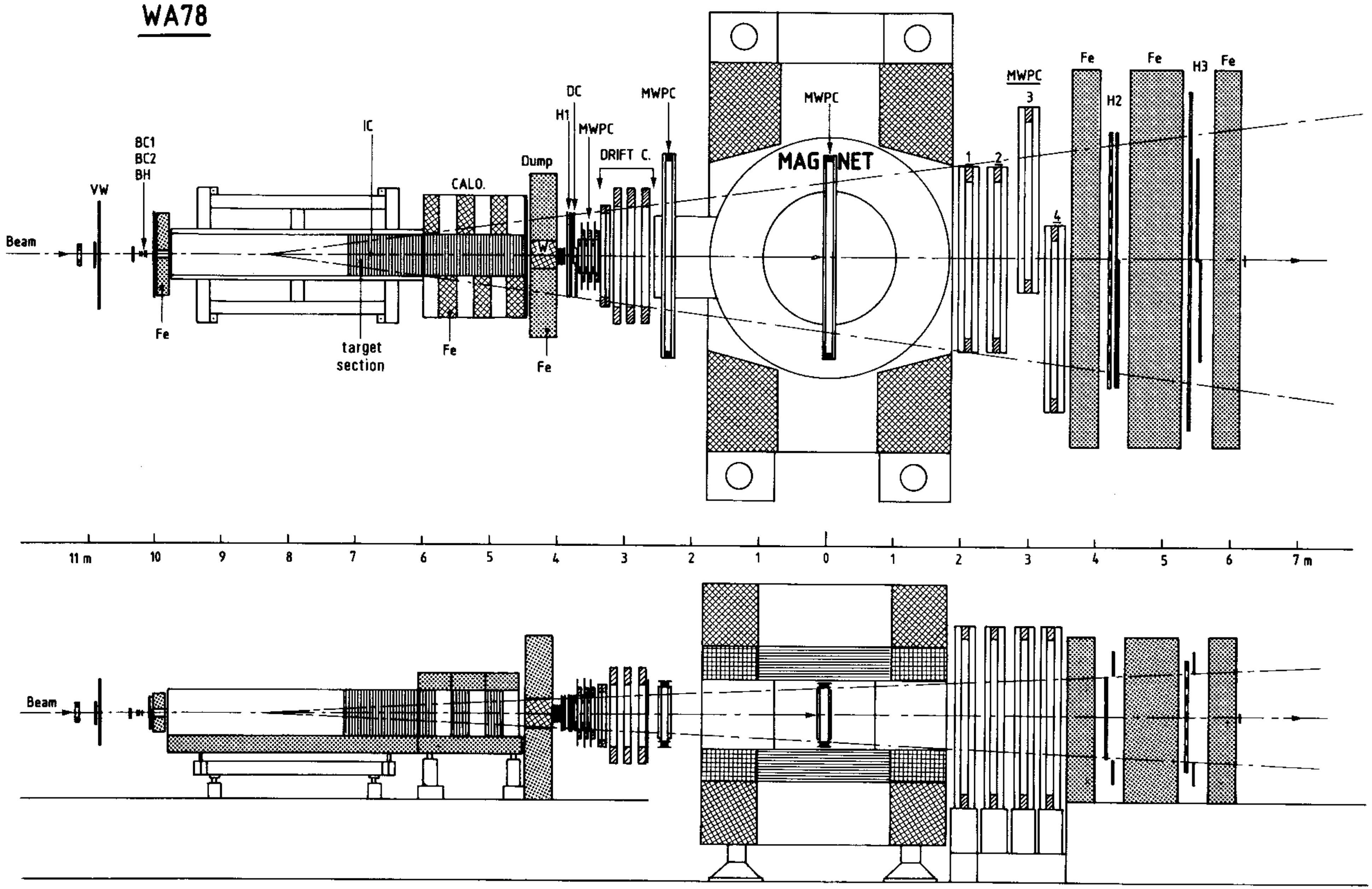
WA78
Beam
VW
BC1
BC2
BH
Fe
IC
target
section
CALO.
Fe
Dump
Fe
W
H1
DC
MWPC
DRIFT C.
MWPC
MWPC
MAGNET
1
2
MWPC
3
4
Fe
H2
Fe
H3
Fe
11 m
10
9
8
7
6
5
4
3
2
1
0
1
2
3
4
5
6
7 m
Beam

Fig. 1

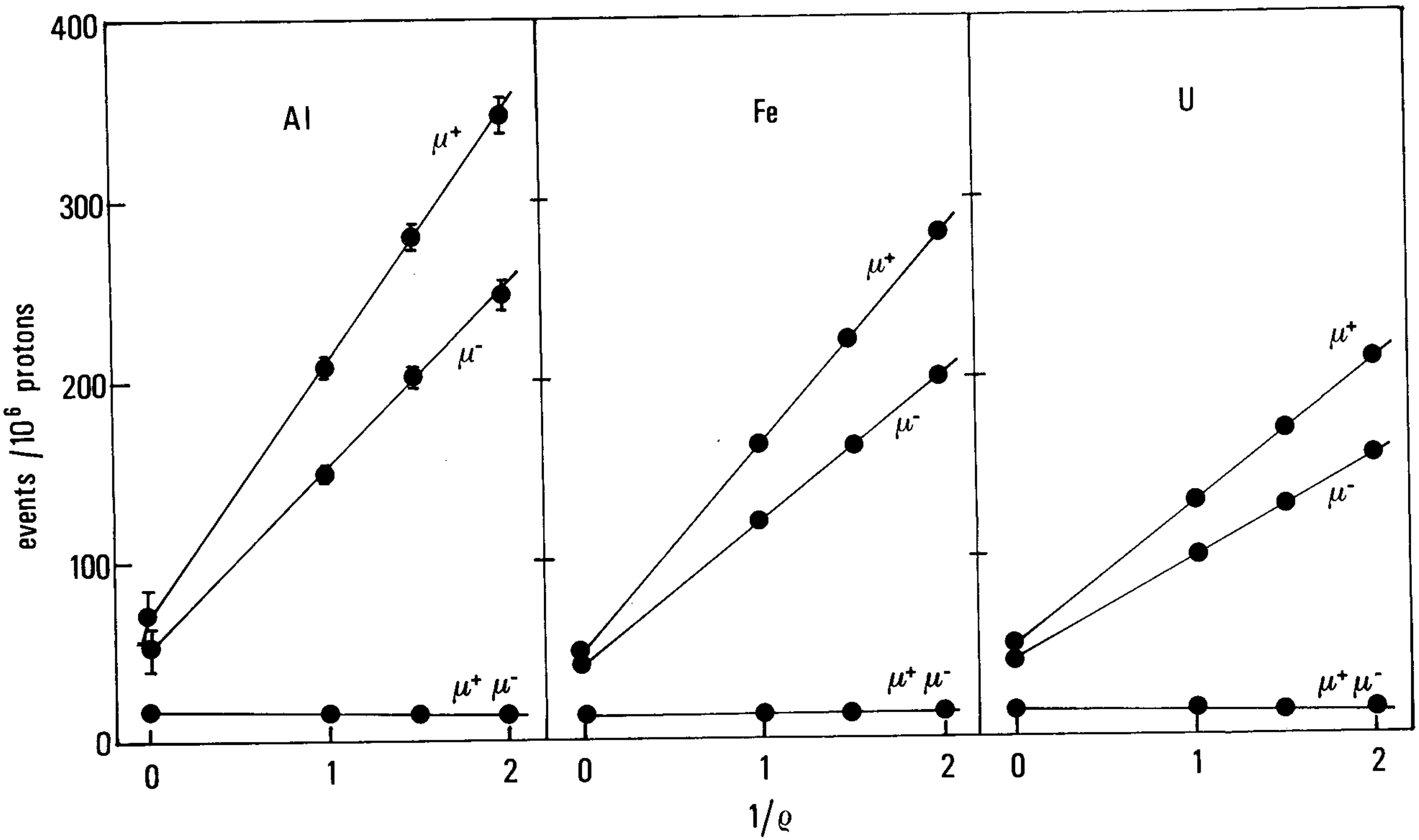

events /10^6 protons
400
300
200
100
0
Al
Fe
U
μ^+
μ^-
$\mu^+ \mu^-$
0
1
2
$1/\varrho$

Fig. 2

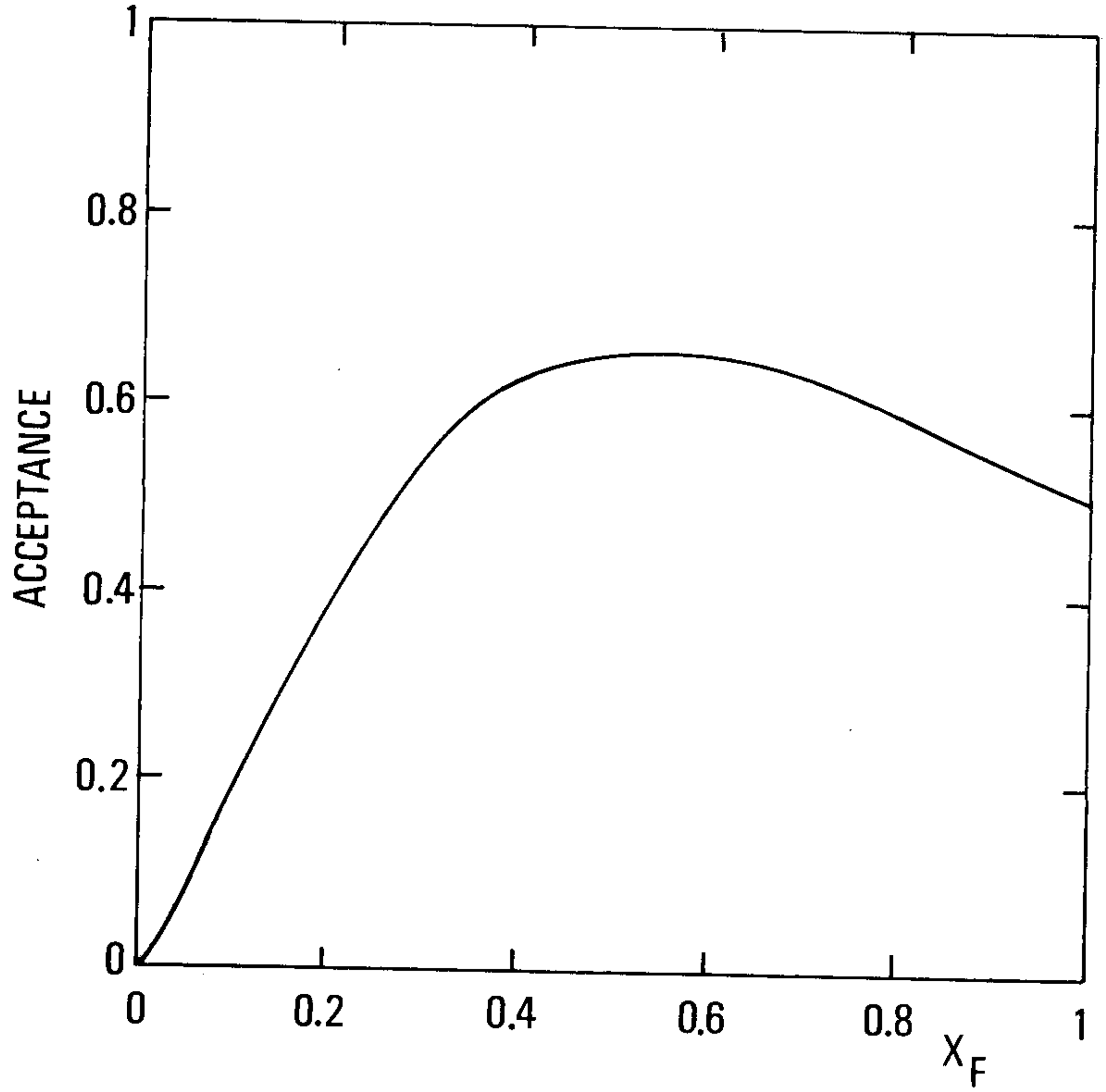

Fig. 3

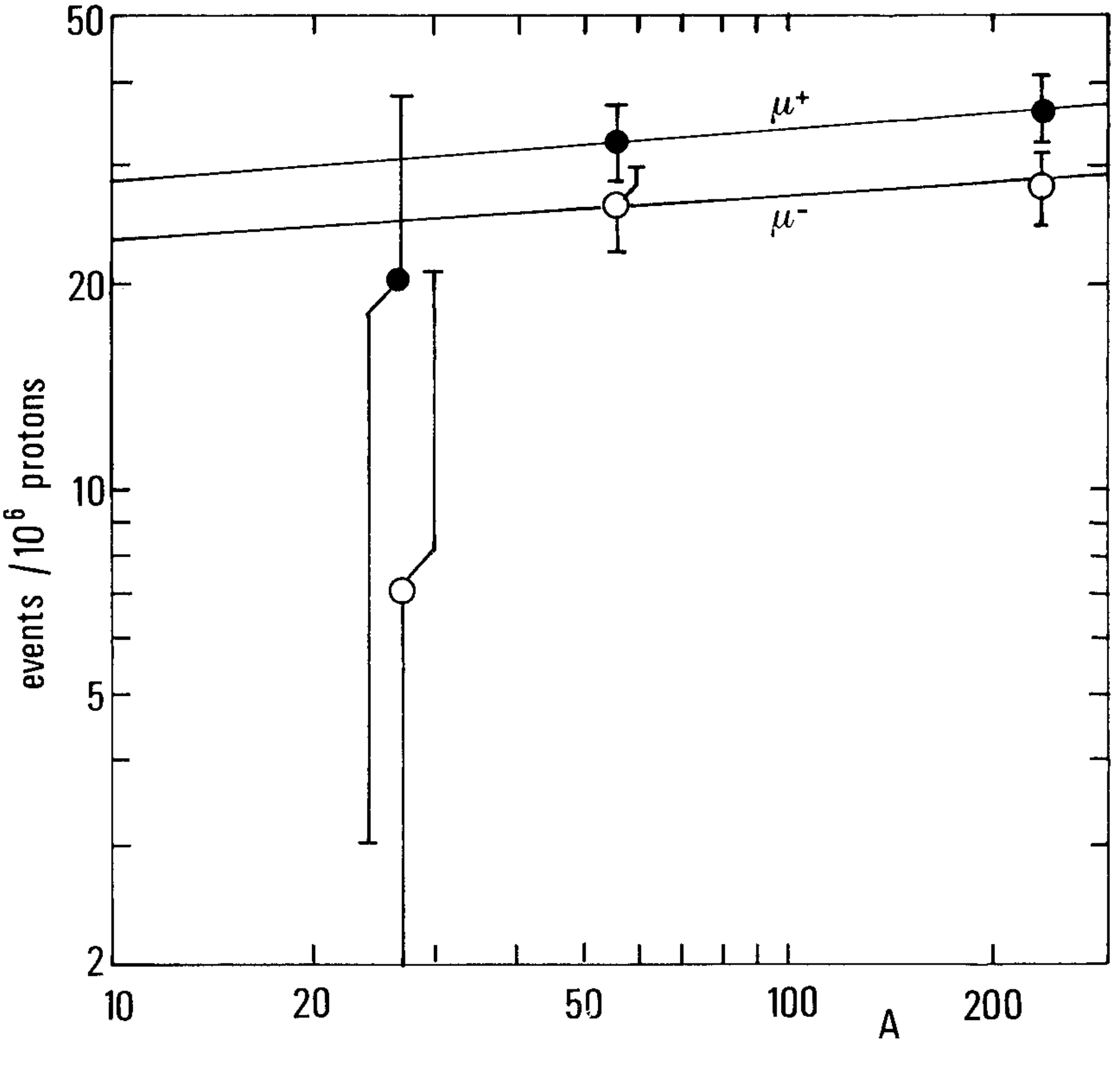

Fig. 4